Self-trapped excitons in SrFCl studied by *ab initio* methods

R. C. Baetzold
Corporate Research Laboratories, Eastman Kodak Company, Rochester, New York 14650-2001

K. S. Song
Department of Physics, University of Ottawa, Ottawa, Ontario, Canada K1N 6N5
(Received 9 November 1992; revised manuscript received 20 July 1993)

Self-trapped excitons (STE's) on the Cl^- or F^- sublattices of SrFCl have been studied using quantum clusters embedded within point ions or self-consistently within shell-model ions. The unrestricted Hartree-Fock method of calculation is used to treat the clusters. Three possible STE's are studied. When the in-plane [100] Cl_2^- STE is displaced from an on-center position the total energy decreases and it becomes basically a one-center species with a hole on one Cl^- ion and the excited electron on the incipient Cl^- vacancy. The Cl-Cl bond length becomes 3.46 Å, reflecting the one-center character of this species. The Cl_2^- out-of-plane STE behaves similarly with displacement in the [111] direction. The F_2^- STE remains as a molecular species with displacement in the [110] direction. The hole becomes localized on the F^- ion nearest the incipient F^- vacancy and on which the excited electron becomes localized. There is a large barrier for electron-hole separation for all of these STE's. The presence of an adjacent halide vacancy allows the electron and hole to separate into a V_K center and an F center without going through an intermediate H center, as occurs in alkali halides.

I. INTRODUCTION

The alkaline-earth fluorohalides (AEH) have shown possible applications in storage phosphor technology.[1-3] In this application, x-ray exposure of a member of this family such as BaFBr creates free excitons that are thought to be mobile. They can become self-trapped excitons (STE), perhaps near a crystal imperfection or impurity, which are thought to produce separately localized electron-hole centers through analogous mechanisms known in alkali halides.[4-6] The electron component is known to be an F center,[7,8] and the hole component is known to be a V_K center below 140 K[9,10] with the appearance of other species such as O^- at room temperature.[11,12] Photostimulation of the exposed phosphor with a He-Ne laser causes recombination of the electron and hole pair with resultant energy transfer to impurity Eu^{2+} ions that undergo luminescence at 390 mm. The purpose of this work will be to study computationally the conversion of the STE to separately localized electron-hole pairs in SrFCl, a representative member of the AEH family of materials.

In alkali halides (AH) the self-trapped exciton has been characterized by a variety of experimental techniques, including resonance Raman scattering[13] and luminescence studies.[14] Only recently has a model been able to explain a variety of these experimental data. This model has been developed computationally,[6,15,16] and through analysis of experimental data by Song and co-workers. The model shows that the STE, while consisting of a halide molecular anion along the [110] axis of AH, is not positioned symmetrically between cations. Rather, the triplet STE is off-center, having achieved an energy lowering of approximately 1 eV (depending upon the material) by movement from the on-center symmetrical site. The halide molecular anion is strongly polarized, having a hole largely localized on the ion located on the back side of the direction of motion and the excited electron localized on the anion vacancy created by the off-center motion. This separately localized electron-hole centers can be considered a close F-H pair. A number of recent *ab initio* Hartree-Fock calculational studies have supported the above model.[16,17] According to this model the close F-H pair can separate further into a stable, well-separated F-H pair with small (0.1 eV or less) activation energy. This has also been supported by a recent calculation.[18] As pointed out above, this model has been thought to apply in the AEH family of materials.

The AEH materials possess a tetragonal layered crystal structure[19] shown in Fig. 1. Here the fluoride ions are close packed, but the larger anions X(are arranged in adjacent layers. Clearly this low-symmetry structure offers many possible orientations and pathways for motion of the STE. We have noted three such choices in Fig. 1 involving the F_2^- molecular anion and two involving the

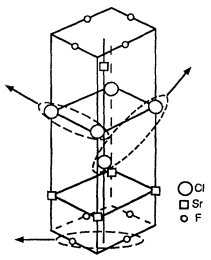

FIG. 1. The unit cell of SrFCl or BaFBr is given. Pathways of various STE motion are sketched. A dashed line designates the hidden edge.

X_2^- molecular anion. These pathways have been probed in earlier work,[20] where one-electron methods have been used to study the STE in BaFBr. In that study, evidence for spontaneous off-center motion of each type of STE was found. The present work applies the Hartree-Fock all-electron method to this problem in AEH, and extends it significantly.

Evidence for the STE has been reported in BaFBr and SrFCl. The absorption and reflection spectra of SrFCl and BaFBr were measured in the vacuum ultraviolet region of the spectrum.[21] Exciton bands have been assigned on the basis of these studies. The halogen spectra are split by spin-orbit coupling. Here the CI or Br free exciton consists of an excited electron bound to a hole localized on the Cl or Br. The Cl exciton appears at 8.74 and 8.86 eV in SrFCl and the Br exciton at 7.64 and 8.15 eV in BaFBr. A maximum has also been reported for the long-wavelength side of the reflection spectra of SrFCl, which is attributed to excitons at intrinsic lattice defects. The F exciton would be expected to absorb at shorter wavelengths. Recent vacuum UV studies[22] have shown peaks for BaFBr reflectivity in the region of 10–15 eV, which are thought to be due to F excitons.

In this paper we study the STE in SrFCl by use of the many-electron Hartree-Fock method. SrFCl is more tractable than BaFBr with the methods we have, but the qualitative patterns for SrFCl should fully extend to BaFBr. Our main objective in this work is to determine the structure of the STE and its relationship to the Frenkel defects. In particular, we confirm that the STE is unstable in the on-center geometry as in the AH. However, in contrast to the latter the STE in SrFCl encounters a substantial energy barrier on the pathway toward well-separated defect pairs. In Sec. II we describe the two embedding procedures we employ to enclose the quantum cluster, and provide details of the basis sets and other input quantities. In Sec. III we provide results of the total-energy calculations for off-center motion of the three possible pathways considered. Details of the geometry and charge distribution of the off-center configurations are provided. We also discuss the possibility of STE migration through a zigzag chain pathway. Finally, we consider the effect of anion vacancies on possible reactions of the STE. In Sec. IV we discuss the relationship of our computational results to experimental results for BaFBr and SrFCl where data exists. Comment on the relevance of these results to phosphor mechanisms is provided.

II. METHOD

The triplet state of the STE is treated at the unrestricted Hartree-Fock (UHF) level. A quantum cluster is chosen to enclose the STE molecular anion. The quantum cluster is embedded within a representation of the remainder of the crystal lattice. Two different representations involving fixed point ions in a spherical array or shell-model cluster ions were employed. The geometry of ions within the cluster is optimized by variation of the positions of specific ions that will be identified. Floating Gaussian orbitals (FGO's) are positioned to provide for possible occupation by the excited electron, as has been shown important in earlier work of Song.[6,15]

Let us recall the three possible excitons shown in Fig. 1. In the case of the STE involving F_2^- we picture the F_2^- molecular anion with a [110] orientation with the excited electron in the region of the molecular anion. We will examine the effect of motion of the molecular anion in the [110] direction. In such cases two FGO's are located on the [110] axis and within 0.4 a.u. of the sites occupied by the ions of the molecular anion in the perfect lattice. Second, we consider the Cl_2^- molecular anion along the [100] axis, which is referred to as the Cl_2^- in-plane STE. Motion of the molecular anion in the [100] direction is considered. In all such models two FGO's are positioned on the [100] molecular axis 0.3 a.u. off the perfect Cl^- sites. Lastly, we consider the out-of-plane Cl_2^- STE consisting of neighboring Cl^- ions arranged along the [111] direction. Motion of the molecular anion along the [111] direction is considered. The two FGO's are positioned on this axis at a distance of 0.5 a.u. from the perfect lattice sites. Unless otherwise specified, the positions of the FGO's are fixed and the exponents fixed at 0.08, as in previous work.[16]

Different sizes and shapes of quantum clusters were required to model the various types of STE's in SrFCl due to its low crystal symmetry. Limitations of reasonable computing times and roughly 250 basis functions restrict the clusters to a size of roughly ten ions. The actual clusters that we employ are shown in Figs. 2 and 3, in which a portion of the remainder of the crystal lattice is also shown. We explain the clusters and the associated optimization procedures in the presence of the fixed-ion embedding scheme first. The Sr_6F_6 cluster in Fig. 2(a) is used to treat the F_2^- STE. The geometry optimization of this cluster proceeds by fixing the positions of the outer ions and allowing the positions of the inner four F^- ions and two central Sr^{2+} ions to vary. The Cl_2^- in-plane STE is treated by the $Sr_2Cl_4F_3$ cluster shown in Fig. 2(b), where the F^- ions and two Cl^- ions on top are fixed, and the positions of the other ions optimized. The Cl_2^- out-of-plane STE was treated by the Cl_6 cluster shown in Fig. 2(c), given with a zigzag orientation along the [110] plane. Here the positions of all six Cl^- ions were optimized in the presence of a short-range Born-Mayer term[23] interacting between the quantum ions and the nearest fixed point-ions. We emphasize that all of the above geometry optimizations are done in the presence of the fixed point ions and utilize the analytic gradients method in the CADPAC (Ref. 24) code. We have used the partial geometry optimization procedure in earlier studies[16,18] of the STE in AH. Compared to full cluster geometry optimization procedures the total energy varies, but the shape of the potential-energy curve as a function of displacement of the STE is unaltered.

The UHF calculation is performed with the CADPAC code.[24] The full-basis sets are (333333|3333|33) (Ref. 25) for Sr^{2+} and 631G for Cl^- and F^- ions. These basis set functions represent the best we could employ within the framework of cluster size and reasonable computing times. The fixed-point embedding array of charges were spherically centered at the midpoint of the on-center STE

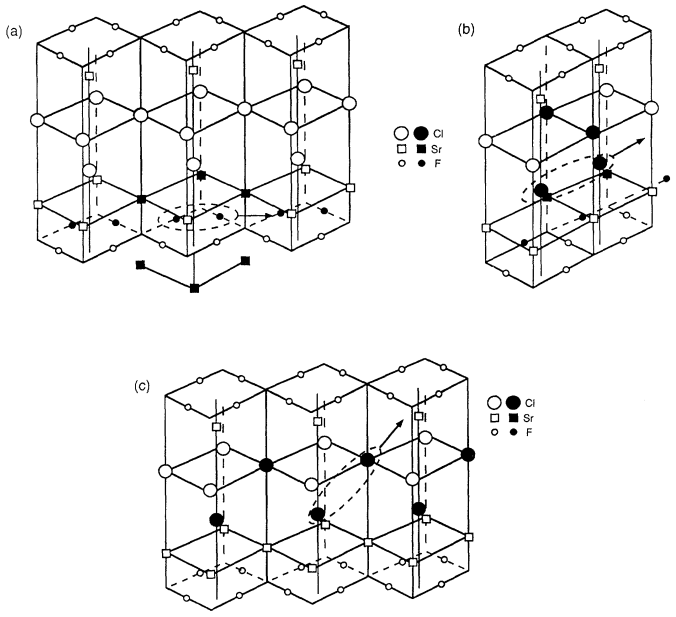

FIG. 2. Clusters employed to treat various STE's are indicated in solid symbols within the unit cells of the SrFCl crystal. The fixed-point-ion embedded calculations employ Sr_6F_6 in (a) to treat the F_2^- STE, and $Sr_2Cl_4F_3$, in (b) to treat the Cl_2^- in-plane STE, and Cl_6 in (c) to treat the Cl_2^- out-of-plane STE. The molecule ion is circles and an arrow indicates the direction of STE motion.

for the three models explained above. The charge of the outermost ions was adjusted to give an array, including the quantum cluster ions, which has neutral charge. The point-ion arrays contain 1128 ions for the F_2^- STE, 1120 ions for the Cl_2^- in-plane STE, and 1018 ions for the Cl_2^- out-of-plane STE.

We now consider the clusters used with the shell-model-embedding scheme. For the F_2^- STE we employ a Sr_6F_4 cluster derived by omitting the two outer F^- ions for the cluster in Fig. 2(a). Here we were successful in performing a geometry optimization with the ICECAP code[26–29] for the positions of the F^- ions. The Cl_2^- in-plane STE was represented by the Sr_8Cl_4 cluster in Fig. 3(a), where the positions of the Cl STE ions and the two

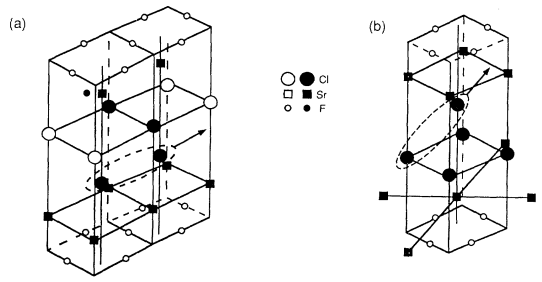

FIG. 3. Clusters used for ICECAP calculations include Sr_8Cl_4 in (a) for the Cl_2^- in-plane STE, and Sr_9Cl_5 in (b) for the Cl_2^- out-of-plane Cl_2^- STE.

closest Sr^{2+} ions were optimized. The Cl_2^- out-of-plane STE was treated by the Sr_9Cl_5 cluster in Fig. 3(b), where we optimized positions of the Cl_2^- molecular anion and the two closest Sr^{2+} ions. While we attempted calculations in which the positions of all cluster ions were optimized, this was not successful because of the loss of symmetry and failure of the calculation. Under full cluster-ion geometry optimization we would expect an energy lowering of both on-center and off-center STE geometries, but not a change in the qualitative behavior of the potential-energy curves.

The methodology using the ICECAP code[26–29] has been developed to achieve a self-consistent coupling of the quantum cluster with the surrounding shell-model ions. This is achieved by expansion of the charge distribution within the quantum and classical parts of the calculation, and the addition of small simulator charges to achieve a fit of multipole moments of the two parts of the calculation. We employ up to quadrupole moments in this work. The norm-conserving Bachelet-Hamann-Schluter pseudopotentials[30] were employed for Sr^{2+} and Cl^- ions. This valence portion of the Sr^{2+} basis of Huzinaga[25] (3) is used for the *s* valence orbitals, the Cl^- basis is (3|21) split from the Huzinaga valence portion, and the F^- basis is (73|33) split from the Huzinaga basis.[25] The classical shell-model two-body potentials for SrFCl are taken from prior work.[23] The shell-model short-range potential parameters are taken independently of the charge state of the ions involved.

In this paragraph we discuss several specific aspects of the UHF method. These include correlation effects, the possibility of spin contamination, and the use of the Mulliken population analysis (MPA) in discussing charge localization. We examined possible correlation effects using Moller-Plesset second-order theory (MP2) to assess the effect of correlation on the potential-energy curves for the three different STE species (F_2^-, Cl_2^- out-of-plane and Cl_2^- in-plane). In order to avoid excessive computations we have performed the MP2 calculations using the ion positions obtained in the UHF study. Automatic geometry optimization using MP2 for these cluster models requires excessive computer resources. We found that although the absolute energy in lowered by roughly 0.1–0.3 eV per electron, depending upon the cluster model, the relative energy changes from the on-center geometry differed by 0.5 eV or less between the UHF calculations with and without MP2. More importantly, however, the shape of the potential-energy curve remained unchanged. Details of this study will be discussed in Sec. III and Table I. Possible spin contamination effects in the UHF method were examined by looking at the expectation value of the spin squared operator for the triplet STE's. Our calculated values for the SrFCl system never exceeded 2.015, and in the course of an off-center displacement the change was very small. For example, using the $Sr_2Cl_4F_3$ cluster the change from on-center to off-center displacement was 2.007–2.004. We consider the close agreement to the value 2.000 to indicate that this is not a major deficiency in our calculations. We evaluated the matter of basis set balance by comparing the results of the two different calculations in this

work. Different basis sets, use of pseudopotential or full electron treatment, and different polarization schemes are represented in the two calculations. The results to be discussed will show excellent agreement on major points which provides justification for the basis sets we employ. Finally, a population analysis inside the quantum cluster is used to provide an indication of the hole and electron localization. This is done with MPA as well as a distributed multipole analysis (DMA).[31] These population analyses, as in all such procedures, are based upon varying sets of definitions and approximations. Some, such as MPA and DMA, are efficient to evaluate, but basis sensitive.[32] Others, such as those based on Bader's work,[33,34] are less basis sensitive, but more computer intensive.[32] We have made a comparison between MPA and DMA for several typical cases and found that they produce comparable results regarding the localization of the hole and excited electron. An example is given in Sec. III C. For convenience of comparison between the two UHF codes employed (CADPAC has both options, but ICECAP has only the MPA option), we have used the MPA option in the rest of the work.

III. RESULTS

A. In-plane Cl_2^- STE

The triplet state of the Cl_2^- in-plane exciton has been examined in on-center and off-center geometries using the fixed-point-ion embedding array. The charges of ions for the two geometries are given in Fig. 4. In the on-center geometry the excited electron is largely on the two FGO orbitals, but also partly on the two nearest Sr^{2+} ions. The Cl_2^- molecular anion has a bond length of 2.923 Å. The two Sr^{2+} ions have moved apart 0.234 Å normal to the molecular anion axis. As the molecular anion is displaced off-center the total energy first drops, then rises (Fig. 5). The equilibrium geometry of the off-center defect has a Cl_2^- molecular anion bond length of 3.461 Å. In this configuration the trailing ion of the molecule has moved 0.21 Å in the [100] direction. Here the electron and hole are strongly polarized. The electron is located on the FGO near the nascent ion vacancy, and the hole is strongly localized on the end of the molecular anion nearest the vacancy. This polarization pattern is very similar to that which is observed in AH crystals.[6,16] The Sr^{2+} ions have moved 0.39 Å away from the Cl_2^- molecule in the normal direction. As we described in Sec. II, we have examined the effect of electron correlation using MP2 theory. In Table I the energies of the UHF and MP2 calculations are given, based on the minimization obtained with UHF. The absolute energy of the on-center geometry is given, followed by energy changes for off-center relaxations. We find that the adiabatic potential curve which shows the pathway of reaction remains stable in shape, but the minimum of the potential can be shifted upward or downward by about 0.5 eV compared to the UHF work, depending upon the species studied. This situation is similar to that in NaF.

TABLE I. Comparison of the UHF total energy with and without MP2 corrections for displacement of the STE from the on-center position. The total energy for each on-center configuration is given in parentheses, and energy changes with displacement are reported.

Displacement (Å)	Sr_2Cl_4 model for Cl_2^- in-plane STE UHF (eV) (−219 802.07)	 UHF+MP2 (eV) (−219 814.41)
0.00	0.00	0.00
0.24	−1.25	−0.57
0.53	−1.09	−0.41
1.06	−0.10	0.03
1.59	0.94	1.02
	Cl_4 model for Cl_2^- out-of-plane STE	
	(−50 027.96)	(−50 040.21)
0.00	0.00	0.00
0.05	0.01	0.01
0.18	0.16	0.17
0.55	1.35	1.81
0.73	2.61	2.93
	F_6 model for F_2^- STE	
	(−16 230.31)	(−16 247.63)
0.00	0.00	0.00
0.37	−0.32	−0.84
0.75	−1.33	−1.72
1.13	−2.10	−2.62
1.50	−2.60	−3.03
1.87	−2.19	−2.73
2.24	4.36	3.36

The result of the ICECAP-type calculation of the in-plane Cl_2^- STE is very similar to the result with the fixed-point-ion embedding array. The charge distribution and polarization pattern is similar to that shown in Fig. 4. In the on-center geometry the bond length of the molecular anion is 2.93 Å and the off-center equilibrium structure has its center of mass displaced by 0.13 Å in the [100] direction. The potential-energy curves for this process are shown in Fig. 5, and there is a strong similarity between the two types of calculation.

B. Out-of-plane Cl_2^- STE

We begin with the fixed-point-ion calculation using the Cl_6 cluster of Fig. 2(c). The Cl^- ions of the quantum

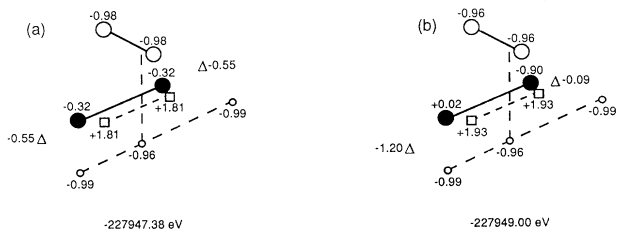

FIG. 4. The Mulliken charge distribution calculated for ions and FGO's (△) is shown for the $Sr_2Cl_4F_3$ cluster [Fig. 2(b)] as computed by the fixed-point-ion embedding method. The on-center (a) and off-center (b) Cl_2^- in-plane STE's are considered with total energies in eV. Ions in the molecule (Cl_2^-) are designated by filled circles.

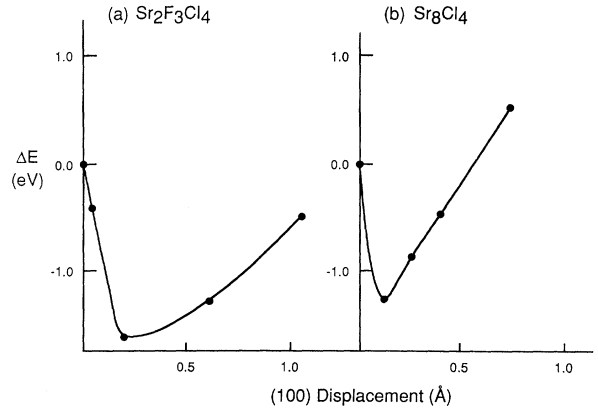

FIG. 5. The total energy (eV) is given for the Cl_2^- in-plane STE vs displacement from the on-center configuration. In (a) the fixed-point-ion calculation for $Sr_2Cl_4F_3$ [Fig. 2(b)] with reference energy −227 947.38 eV is shown. In (b) the ICECAP calculation for Sr_8Cl_4 [Fig. 3(a)] is shown with reference energy −1592.41 eV.

cluster interact with the nearest-neighbor Sr^{2+} ions through Born-Mayer terms. In the on-center case the Cl_2^- molecular bond length is 2.78 Å with the Mulliken charge distribution giving a hole shared equally on the two Cl^- ions in the molecule. Off-center motion along the direction of the molecular axis gives an energy minimum 0.6 eV below the on-center case. The center of the molecule has moved 0.42 Å at this point, and the bond length of Cl_2^- is 2.92 Å. The Mulliken charge gives a hole predominantly on the trailing ion in the molecule with an electron on the FGO nearest this ion. The energy of those configurations may be compared to the energy of the one-center configuration we obtained. Here at the energy minimum one Cl^- ion is displaced by 0.33 Å along the *c* axis into the double layer. The total energy of this configuration is 1.17 eV lower than the on-center case. The charge distribution shows the hole localized on the displaced Cl^- ion and the excited electron in the FGO near its original lattice site. Table I presents potential-energy variations obtained with MP2.

We also treated the out-of-plane Cl_2^- STE using models including Sr^{2+} ions. The Sr_9Cl_5 cluster in Fig. 3(b) was employed. A sketch of the charge distribution of the one-center out-of-plane STE, as treated by ICECAP, is shown in Fig. 6. The hole is almost entirely on one Cl^- ion with a small amount on the two nearest Cl^- ions. The excited electron is localized largely on the one Sr^{2+} ion. The energy of this one-center species is 1.28 eV lower than the on-center defect. In this calculation off-center displacement of the molecular anion in the [111] direction of the on-center exciton led to an increase in energy and was not studied further. Thus the one-center character of the out-of-plane Cl exciton is similar to our findings in the fixed-point-ion calculations, but in this calculation the excited electron becomes localized on Sr^{2+} ions.

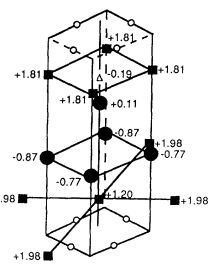

FIG. 6. The Mulliken charge distribution on ions and FGO's (△) is shown for the Sr_9Cl_5 cluster [Fig. 3(b)]. The ICECAP calculation for the one-center out-of-plane Cl_2^- STE is considered.

C. F_2^- STE

The Sr_6F_6 cluster [Fig. 2(a)] embedded in fixed-point charges has been used to study off-center motion of the triplet STE. The potential-energy curve is shown in Fig. 7. With off-center displacement the total energy first decreases, then increases. The energy minimum is rather shallow of the order of 0.1 eV at a displacement of 0.53 Å. As will be discussed in Sec. IV, an energy barrier of this magnitude is outside the reliable accuracy of the present *ab initio* calculations. We conclude that this result indicates a flat potential surface. The F-F bond length in the off-center equilibrium position is 1.995 versus 2.179 Å in the on-center position. The Sr^{2+} ions have moved in the *c* direction by 0.13 Å. A sketch of the charge distribution in the on-center and off-center geometries is shown in Fig. 8. In the on-center configuration, the excited electron is largely on the Sr^{2+} ions. With off-center motion it becomes localized on the floating Gaussian nearest the incipient halide vacancy. The hole is localized on the fluoride ion nearest this vacancy.

Table I gives the energies of this system obtained with

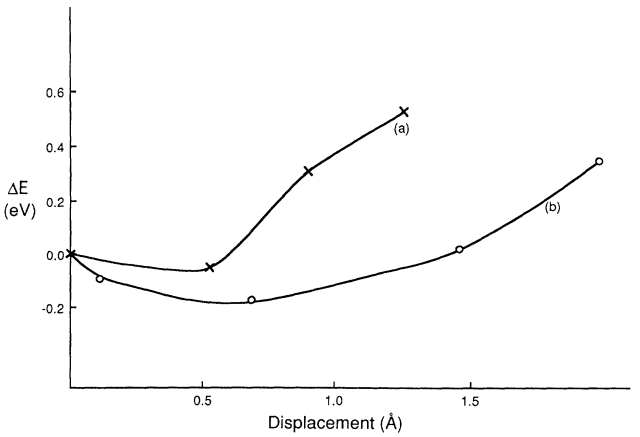

FIG. 7. The change in total energy of the F_2^- STE is shown vs displacement in the (110) direction from the on-center configuration. The Sr_6F_6 cluster [Fig. 2(a)] is treated by the fixed-point-ion embedding method in (a), where the reference energy is −525 666.48 eV. The corresponding calculations for the Sr_2F_6 cluster [formed by omitting the four outermost Sr ions of Fig. 2(a)] using ICECAP gives the curve in (b) with reference energy −5400.42 eV.

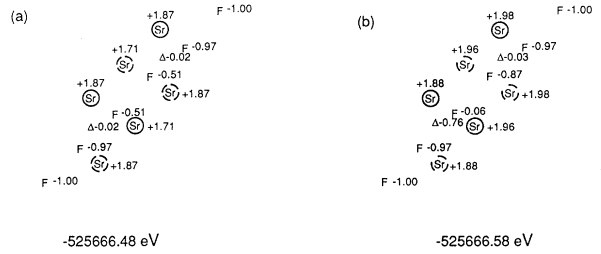

FIG. 8. The Mulliken charge distribution on ions and FGO's (△) is shown of the Sr_6F_6 cluster [Fig. 2(a)]. The fixed point-ion embedding calculation is used to treat the on-center case in (a) and the off-center case in (b) of the F_2^- STE. The Sr ions enclosed in solid circles or dashed circles are above or below the planes containing the F^- ions, respectively.

and without MP2 correlation corrections. As with other cases presented above, the potential curve for off-center relaxation is not modified in shape by considering correlation, although the depth of the minima changes by about 0.5 eV. As was briefly discussed in Sec. II above, we have made a comparison of population analyses obtained by MPA and DMA, using the CADPAC code. A typical result is shown in Table II for the present system, which is also given in Fig. 8. It appears first that the electron populations on the ions other than the central fluorine ions are practically the same in the two methods. The most interesting points for us are the charges on the two FGO's and the central fluorine ions on which the hole is self-trapped. There are some numerical differences in the two methods, but regarding the important point of the hole and excited electron attracting each other in the off-center geometry there is good agreement. The use of diffuse FGO's to enhance the basis for the excited electron presents problems due to the overlap of charges. This is how the basis dependence arises in many population analyses. In all cases we studied, the basic point of hole and excited electron correlation was observed, as would be expected from other works on the STE.[16–18]

TABLE II. Comparison of Mulliken and distributed multipole analysis populations for Sr_6F_6 clusters in Fig. 8.

	On-center		Off-center	
Ion	Mulliken	Multipole	Mulliken	Multipole
FGO	−0.02	−0.16	−0.03	−0.03
FGO	−0.02	−0.16	−0.76	−1.37
F	−0.51	−0.46	−0.07	+0.07
F	−0.51	−0.46	−0.87	−0.87
F	−0.97	−0.98	−0.97	−0.97
F	−0.97	−0.98	−0.97	−0.97
F	−1.00	−1.00	−1.00	−1.00
F	−1.00	−1.00	−1.00	−1.00
Sr	+1.87	+1.91	+1.96	+2.03
Sr	+1.87	+1.91	+1.96	+2.03
Sr	+1.71	+1.77	+1.98	+1.98
Sr	+1.71	+1.77	+1.98	+1.98
Sr	+1.87	+1.91	+1.88	+2.04
Sr	+1.87	+1.91	+1.88	+2.04

The treatment of the F_2^- STE using the ICECAP method uses the Sr_6F_4 cluster. Off-center motion causes first a decrease in energy, and then an increase in energy. The potential curve is shown in Fig. 7, and the charge distributions on the ions is similar to that shown in Fig. 8. The on-center case gives the excited electron as largely on the Sr ions. The hole is shared equally by the two ions in the molecular anion. Off-center motion causes a localization of the excited electron largely on the floating Gaussian near the F^- vacant site. The pattern of energetics and charge polarization that emerges from this calculation is like that from the fixed-point-ion embedded calculation.

D. Effect of halide vacancies

The results of STE off-center motion by and large have given a situation where the electron and hole become partially separated. As the potential-energy curves show, large barriers are then encountered for further separation of the electron and hole. In this regard the SrFCl STE seems quite unlike the STE in AH, where dissociation can take place with barriers as small as 0.1 eV, as deduced from thermally activated *F*-center conversion of the STE.[6] We have considered the effect that a halide ion vacancy might have on electron-hole separation. A Sr_8Cl_6 cluster containing the one-center out-of-plane STE and one Cl^- vacancy is considered. The vacancy is at various sites on the Cl^- sites of the cluster and the ICECAP calculation is performed. One FGO is placed on the vacant site. The energy and charge distribution are shown in Fig. 9 for various placements of the vacancy/FGO. In Fig. 9(a) results are shown for a UHF solution where the hole is on one end Cl^- ion and the Cl^- vacancy is at the opposite end. The excited electron

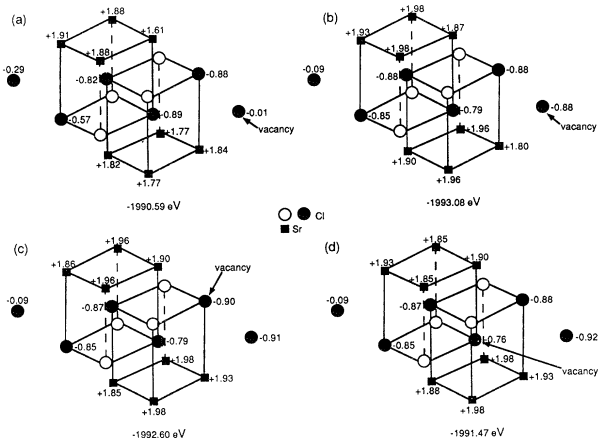

FIG. 9. The Mulliken charge distribution and energy are shown for a Sr_8Cl_6 cluster treated by ICECAP. The Cl^- quantum ions are in solid symbols, and one Cl^- vacancy replaced by an FGO is indicated. A hole is localized on one end of the cluster by moving the Cl^- ion along the *c* axis into the double layer to achieve our energy minimum. This ion is fixed in position, and the vacancy is placed at different distances from the hole in (a), (b), (c), and (d). The different converged solution in (a) and (b) results from different starting eigenvectors.

is primarily on the Sr^{2+} ions. It is also possible to converge to a different solution for the same geometry and basis sets by starting with different initial vectors. The second solution shown in Fig. 9(b) has the vacancy with a trapped electron at the FGO. Now the excited electron has become an *F* center. The energy of this solution is approximately 2.5 eV below the first solution, indicating increased stability for the separated electron and hole. Intermediate cases are considered in Figs. 9(c) and 9(d) where the Cl vacancy is closer to the hole. In these cases an *F* center is formed at the vacancy and the energy is intermediate between the two limiting cases. This behavior is interpreted to indicate that the presence of a Cl^- vacancy allows the electron and hole to separate.

The effect of F^- vacancies on the F_2^- exciton has also been studied using the Sr_6F_4 model with the ICECAP method. A lowering of energy has been found for population of the FGO located on F^- vacancy, and so the same effect discussed above for Cl_2^- excitons is believed to operate for F_2^- excitons.

E. Absorption energy

We can compare the absorption and emission energies calculated for SrFCl using the fixed-point-ion embedding method. The absorption energy is calculated for the open-singlet state of the perfect cluster. The absorption energy is taken as the difference in energy of the open singlet and the perfect cluster ground state. The emission energy is taken as the difference in energy of the most stable off-center triplet STE and the ground state with the same ion positions. The experimental absorption energies are 8.8 eV for the Cl exciton, and estimated to be 10–11 eV for the F exciton. These data are shown in Table III. There is a reasonable level of agreement between calculation and experiment. Comparison of the emission and absorption energies show that the Stokes shift is small. This behavior is consistent with a small off-center displacement based upon our computations for AH materials.[18]

IV. DISCUSSION

There are interesting parallels in the behavior of the STE, which we compute in SrFCl and AH.[16,18] In both cases our many-electron Hartree-Fock calculations predict a spontaneous off-center motion of the STE. The STE in SrFCl has a molecular anion structure for F_2^-, but for Cl_2^- the bond length is increased (to 3.46 Å) over the bond length of the Cl_2^- STE in NaCl (2.73 Å).

TABLE III. Computed absorption and emission energies for STE in SrFCl.

Exciton	Absorption energy (eV) Calculated free-exciton open singlet	Experiment (Ref. 21)	Emission energy (eV)
F	13.5	10–11	10.6
Cl in-plane	9.8	8.8	6.2
Cl out-of-plane	11.5	8.8	8.0

In the off-center configuration a one-center model may be a better description of the Cl^- STE. In both the F_2^- and Cl^- STE the polarization pattern is the same as in the AH crystals. The electron becomes well localized on the incipient halide ion vacancy, and the hole becomes localized on the halide ion nearest the vacancy. Qualitatively this pattern of behavior is similar to that computed by the extended ion method for BaFBr.[20] We note a suggestion that the F_2^- exciton is out-of-plane has appeared in a report on luminescence.[25]

There are some significant differences in behavior of the STE in SrFCl and AH crystals. In the AH crystals we obtained[18] virtually no barrier for separation of the electron and hole. In fact, the potential surface obtained was flat to within the accuracy of the method used, which we estimate to be 0.2 eV. Large barriers are encountered for this process in SrFCl. A primary difference in the crystal structures of the two classes of materials probably accounts for this different behavior. In AH systems having the NaCl lattice, the existence of a (110) row of halide ions is important in promoting the efficient bond-switching sequence of the halide molecular anion (X_2^-) and leads to a low barrier for *F-H* pair separation. On the other hand, the present material is similar to fluorites such as SrF_2. It is well known from electron paramagnetic resonant (EPR) data[36] and from theoretical calculations[37] that the STE in the fluorites is a nearest neighbor *F-H* pair aligned along the [111] axis. This means that the STE undergoes a relaxation consisting of axial translation at the beginning along the [100] axis superimposed with a rotation near the end of the trajectory. Further separation of the STE into a second-neighbor *F-H* pair and so on involves bond switchings mediated by rotations. Although the SrFCl crystal structure is more complex than fluorite, it is possible that rotational components after the initial translational components considered here could lead to a lower barrier for separation. Nevertheless, halide ion vacancies near the STE promote this separation. Thus in this mechanism in the SrFCl crystal, *H* centers, which are known in AH crystals, would not be formed. In this regard, we would like to point out that no experimental evidence for forming *F-H* pairs in *X* irradiation of BaFBr at low temperature has been found with EPR or ODEPR.[11] The STE plus vacancy complex would decay to an *F* center plus V_K center, as observed experimentally.[11]

It is most likely that the STE in BaFBr has similarities to the STE in SrFCl. Ion vacancies on the Br^- or Cl^- sublattices are expected to predominate over F^- vacancies based upon atomistic calculations.[23,38] Thus these point defects should be present and permit the STE to dissociate. It is also quite possible that the free exciton becomes trapped near a vacancy leading to the dissociation mechanism we have discussed.

Our treatment of the STE in SrFCl is a comprehensive calculation for this low-symmetry structure material. We have tested several aspects of the calculation in AH and AEH materials. The cluster size chosen represents the largest possible to enclose the STE and yet permit an adequate basis set on each ion. We compared the results of two different types of UHF calculation employing

different basis sets and use of full electron versus pseudopotential methods and yet found similar potential energy curves in Figs. 5 and 7. Similar agreement has also been noted in earlier studies[16,18] in AH. We believe that the present calculations show clearly that the STE's initially undergo a symmetry-breaking axial relaxation leading to a separation of the electron and hole. As we have mentioned at several places above and in Ref. 18, despite the tremendous progress in *ab initio* Hartree-Fock studies of defects in crystals, a number of limitations exist at present. They are the embedding procedure, the optimization of the basis, the use of pseudopotentials, the treatment of correlation effects, and finally the limit in the computational resources. Overall, we feel that in the best situations dealing with the STE we have studied so far, the case of AH such as NaF, the inaccuracy we incur is larger than the experimental thermal activation energy, which is of the order of 0.1 eV. It is for these reasons that the goal of the present work, and others of similar nature, is to determine some basic features of the localized excitations such as the off-center relaxation leading to a possible separation of the hole and electron centers.

[1]G. W. Luckey, US Patent No. 3,859,527 (7, January, 1975).
[2]G. Amemiya and J. Miyahara, Nature **336**, 89 (1988).
[3]K. Takahashi, K. Kohda, and J. Miyahara, J. Lumin. **31**, 266 (1984).
[4]D. Pooley and W. A. Runciman, J. Phys. C **3**, 1815 (1970).
[5]H. Rabin and C. C. Klick, Phys. Rev. **117**, 1005 (1960).
[6]K. S. Song, C. H. Leung, and R. T. Williams, J. Phys. C **1**, 683 (1989).
[7]R. U. Bauer, J. R. Niklas, and J.-M. Spaeth, Phys. Status Solidi B **118**, 557 (1983).
[8]J. R. Niklas, G. Herder, M. Yuste, and J.-M. Spaeth, Solid State Commun. **26**, 169 (1978).
[9]M. Yuste, L. Taurel, M. Rahamani, and D. Lemoyne, J. Phys. Chem. Solids **37**, 961 (1976).
[10]T. Hangleiter, F. K. Koschnick, J.-M. Spaeth, R. H. D. Nuttall, and R. S. Eachus, J. Phys. C **2**, 6837 (1990).
[11]R. S. Eachus, W. G. McDugle, R. H. D. Nuttall, M. T. Olm, T. Hangleiter, F. Koschnick, and J.-M. Spaeth, J. Phys. C **3**, 9327 (1991); **3**, 9339 (1991).
[12]F. K. Koschnick, J.-M. Spaeth, R. S. Eachus, W. G. McDugle, and R. H. D. Nuttall, Phys. Rev. Lett. **67**, 3571 (1991).
[13]K. Tanimura, T. Suzuki, and N. Itoh, Phys. Rev. Lett. **68**, 635 (1992).
[14]K. Kan'no, K. Tanaka, and T. Hayashi, Rev. Solid State Sci. **4**, 383 (1990).
[15]K. S. Song and C. H. Leung, J. Phys. C **1**, 8425 (1989).
[16]R. Baetzold and K. S. Song, J. Phys. C **3**, 2499 (1991).
[17]A. L. Shluger, N. Itoh, V. E. Puchin, and E. N. Heifets, Phys. Rev. B **44**, 1499 (1991).
[18]K. S. Song and R. C. Baetzold, Phys. Rev. B **46**, 1960 (1992); R. C. Baetzold and K. S. Song, *ibid.* **97**, 1199 (1993).
[19]B. W. Liebich and P. Nicollin, Acta. Crystallogr. Sec. B **33**, 2790 (1977).
[20]R. C. Baetzold, Phys. Rev. B **40**, 3246 (1989).
[21]E. Nicklaus, Phys. Status Solidi A **53**, 217 (1979).
[22]H. H. Rüter, H. V. Seggern, R. Reininger, and Y. Saile, Phys. Rev. Lett. **65**, 2438 (1990).
[23]R. C. Baetzold, J. Phys. Chem. Solids **50**, 915 (1989).
[24]R. D. Amos and J. E. Rice, *CADPAC: The Cambridge Analytical Derivatives Package* (Cambridge University Press, Cambridge, 1989), Issue 4.2.
[25]S. Huzinaga, *Gaussian Basis Sets for Molecular Calculations* (Elsevier, New York, 1984).
[26]J. M. Vail, A. H. Harker, J. H. Harding, and P. Saul, J. Phys. C **17**, 3401 (1984).
[27]J. H. Harding, A. H. Harker, P. B. Keegstra, R. Pandey, J. M. Vail, and C. Woodward, Physica B **131**, 151 (1985).
[28]R. Pandey and A. B. Kunz, Phys. Rev. B **38**, 10150 (1988).
[29]J. M. Vail, J. Phys. Chem. Solids **51**, 589 (1991).
[30]G. B. Bachelet, D. R. Hamann, and M. Schluter, Phys. Rev. B **26**, 4199 (1982).
[31]A. J. Stone, Chem. Phys. Lett. **83**, 233 (1981).
[32]A. J. Stone and M. Alderton, Mol. Phys. **56**, 1047 (1985).
[33]R. F. W. Bader, S. G. Anderson, and A. J. Duke, J. Am. Chem. Soc. **101**, 1389 (1979).
[34]D. L. Cooper and N. C. J. Stutchbury, Chem. Phys. Lett. **120**, 167 (1985).
[35]M. K. Crawford, L. H. Brixner, and K. Somaiah, J. Appl. Phys. **66**, 3758 (1989).
[36]P. J. Call, W. Hayes, and M. N. Kabler, J. Phys. C **8**, L60 (1975).
[37]M. Adair, C. H. Leung, and K. S. Song, J. Phys. C **18** L909 (1985).
[38]R. C. Baetzold, Phys. Rev. B **36**, 9182 (1987).